RSC Advances

ROYAL SOCIETY OF CHEMISTRY

www.rsc.org/advances

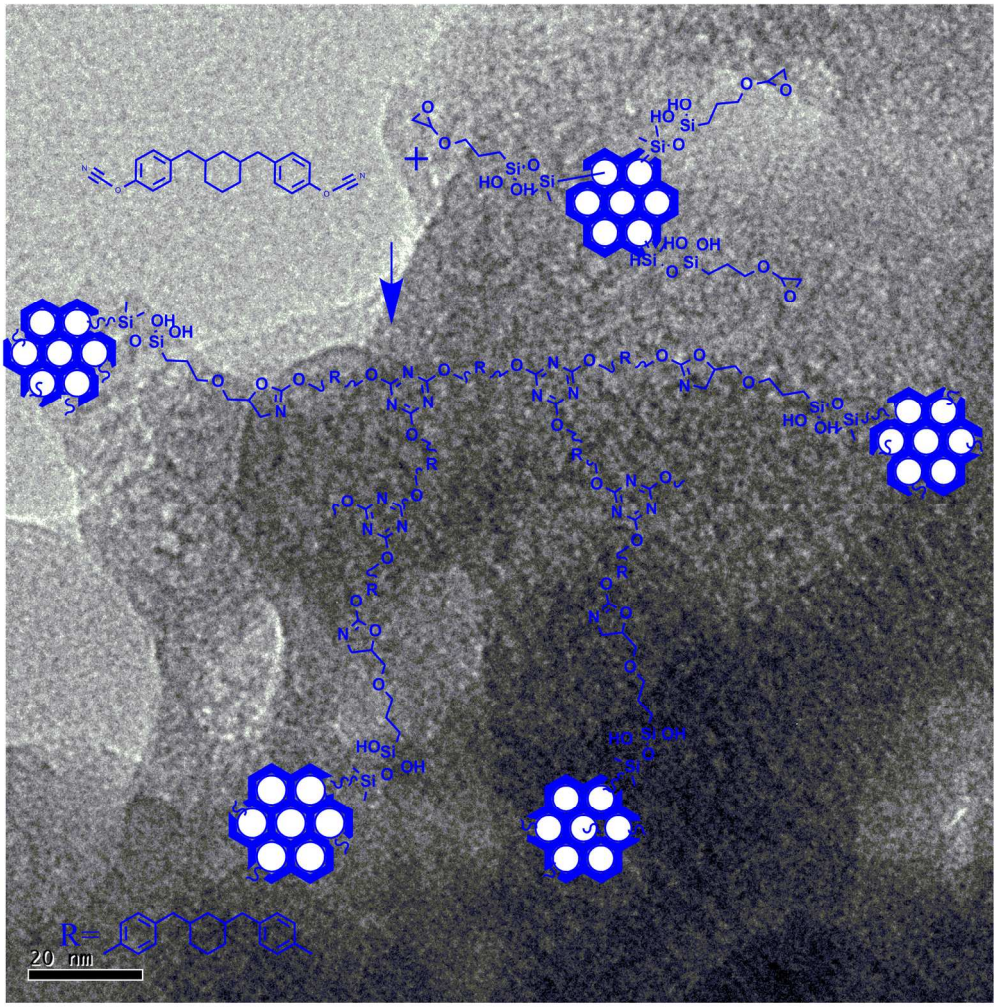

170x171mm (300 x 300 DPI)

Studies on FMCM-41 reinforced cyanate ester nanocomposites for low k applications

Mathivathanan Ariraman, Ramachandran Sasi kumar and Muthukaruppan Alagar*

*Polymer Composites Lab, Department of Chemical Engineering, A.C.Tech, Anna University, Chennai-600 025, India. E-mail: mkalagar@yahoo.com

Abstract

The continual development of microelectronics needs insulation materials with lower value of dielectric constant (low k). To accomplish this, a new type of cyclohexyl branched aliphatic chain bridged cyanate ester has been developed by the synthesis of chalcone from 4-hydroxybenzaldehyde and cyclohexanone, and followed by the reduction. Cyanate ester nanocomposites have been developed by polymerizing cyanate ester monomer reinforced with the varying weight percentages of glycidyl silane functionalized mesoporous MCM-41 (FMCM-41). Subsequently, the monomer and polymer composites were characterized by the spectral analysis of FTIR (Fourier transform infrared), ^{1}H and ^{13}C NMR (nuclear magnetic resonance) spectroscopy. The thermal properties were carried out by TGA (thermogravimetric analysis), DSC (differential scanning calorimetric), and morphological studies were carried out by SEM (scanning electron microscopy) and HRTEM (high resolution transmission electron microscopy) respectively. The HRTEM images clearly indicate the existence of pores, which were responsible for contributing to the reduction of value of dielectric constant. The dielectric properties were measured by broadband dielectric spectrometer. From the dielectric studies it was inferred that 10 wt % of MCM-41 reinforced BCC polymer composites exhibits the lowest value of dielectric constant of 1.98 at 1MHz.

Key words: cyanate ester, functionalized MCM-41, porous structure, dielectric constant.

Introduction

The microelectronics industries were continuously trying to find new technological solutions to the reduction of resistance-capacitance (RC) time delay, low power consumption, and reduced 'cross-talk' between nearby interconnects and to keep pace with the trend of increasing device densities in ultra-large-scale integrated (ULSI) circuits[1]. Generally,

microelectronic integrated circuits consist of interconnect wires which were insulated by the dielectric materials with the intra and interlayer capacitance[2]. In order to reduce the capacitance, it is essential to replace the present insulating materials by the introduction of thin film of low dielectric materials (< 2.2)[3]. There are two main routes normally used to reduce the dielectric constant: 1) by the preparation of polymer nanocomposites with porous silica materials such as polyhedraloligomericsilsesquioxane (POSS)[4], SBA-15[5], MCM-41[6], etc, and 2) by the introduction of less polar aliphatic groups into the skeleton[4]. Thus, the incorporation of porous materials into the polymers significantly reduces the dielectric constant of the polymer composites because the intrinsic air/vacuum has a dielectric constant of ~1[7]. Subsequently, thermally stable dense silica materials drastically increase the thermal stability of the polymer composites. In addition, the existence of less polar functional groups strongly reduces the dielectric constant of the matrix due to the reduction of polarization throughout the matrix which in turn resulting in lowering the capacitance between the electrodes[8]. The ratio of the permittivity of a substance to that of free space is called as Dielectric constant (κ) or relative permittivity (ε_r). A material containing non polar components, which are creating less electric dipoles (e.g. non polar chemical bonds) and has a decreased dielectric constant. The dipole formation is a result of electronic polarization (displacement of electrons), distortion polarization (displacement of ions), or orientation polarization (displacement of molecules) in an alternating electric field. These phenomena have characteristic dependencies on the frequency of the alternating electric field, giving rise to a change in the real and imaginary part of the dielectric constant between the microwave, ultraviolet, and optical frequency range[1,9]. The less polar aliphatic chains inherently reduces the dipoles between the electrodes and significantly reduces the value of dielectric constant.

Networked polymer matrices such as polyimide[10], polybenzoxazine[5], PEEK[11], and cyanate ester[3] were frequently reported as low k materials. Among these the cyanate ester (CE) resin systems draw an increasing attention due to their unique properties such as good thermal and mechanical properties, high glass transition temperature (Tg), radiation resistance, excellent metal adhesion, compatibility with carbon fiber reinforcements, high flame retardant, low moisture uptake and excellent electrical insulation behavior[12]. Moreover, these outstanding performances of CE resin make them as an excellent material for radiation resistant and high temperature applications in aerospace, adhesives and sealants for microelectronics[13]. A cyanate

ester resin is a class of thermosetting polymers and can be prepared by the thermal treatment of monomer in the absence of any catalyst. It is well known that the cyanate esters can easily combined with epoxy resin through covalent bond to form oxazoline five membered rings with low curing temperature. It can also be self polymerized to obtain cross linked polycyanurate with six member triazine rings[14]. The polycyanurate segment contributes to an improved thermal stability with superior mechanical toughness than those of other thermosetting polymers. Furthermore, the existence of less polar aliphatic, oxazoline, and triazine influence the reduction of the value of dielectric constant of the materials. Recently, porous silica materials incorporated cyanate ester polymer nanocomposites have been reported, it can be seen that the 10% OG-POSS reinforced bisphenol cyanate ester nanocomposites exhibits the value of dielectric constant of 2.4 which is lower than that of neat CE matrix[8]. In addition, 15% glycidyl silane functionalized mesoporous silica reinforced polycyanurate exhibit the lower values of dielectric constant (2.11) than that of neat matrix[3]. Hence, reinforcing the varying weight percentages of porous silica and the existence of less polar aliphatic long chain in the polymer composites are vital parameters considered to reduce the dielectric behavior of insulating materials.

In this context, In the present work we have developed cyclohexyl branched aliphatic long chain bridged phenolic cyanate ester and which was cured and reinforced with the varying weight percentages of gycidyl silane functionalized mesoporous MCM-41and were characterized and reported. It was observed that silane the increasing weight percentages of FMCM-41 strongly influenced in the reduction of value of dielectric constant and also significantly enhanced the thermal stability of the cyanate ester polymer nanocomposites.

Experimental

Materials

Analytical grades of 4-hydroxybenzaldehyde, cyclohexanone, cyanogen bromide (CNBr), triethylamine (TEA), acetic acid, sulfuric acid and solvents were purchased from SRL, India. High purity sodium trisilicate, cetyl trimethylammonium bromide (CTAB), 3-(glycidyloxypropyl)trimethoxysilane **(**GPTMS) and 10% Pd/C were purchased from Sigma-Aldrich and were used as received without further purification.

Synthesis of (2E,6E)-2,6-bis(4-hydroxybenzylidene)cyclohexanone (BHC)

(2E,6E)-2,6-bis(4-hydroxybenzylidene)cyclohexanone (BHC) was synthesized as per the reported procedure[15]. To a solution of 4-hydroxybenzaldehyde in the mixture of acetic acid and catalytic amount of sulfuric acid, and cyclohexanone were added and stirred for 48h at room temperature. After the completion of reaction (monitored by TLC), ice cold water was added to the reaction mixture and resulting precipitate was filtered and washed several times with water to yield 90% off brown solid as final product.

Synthesis of 4, 4'-(cyclohexane-1,3-diylbis(methylene))diphenol (CDD)

To a stirred solution of BHC in methanol, 10% Pd/C was added under N_2 atmosphere and subsequently changed the reaction atmosphere with hydrogen and stirred for 48h at RT. After the completion of reaction, the reaction mixture was filtered through celite and the filtrate was concentrated under reduced pressure. Further the purification procedure is as follows; the resulting product was dissolved with little amount of methanol and cooled with crushed ice, followed by the addition of cold water to obtain the precipitate. The precipitate was filtered and washed several times with water and dried for 12h at 70°C to yield 90% pale pink solid product.

^{1}H NMR (DMSO-d_6, δ, ppm): 9.14 (-OH), 6.93-6.61 (aromatic protons), 2.63-2.46 (methylene proton), 1.89-1.16 (cycloaliphatic protons).

Synthesis of 1, 3-bis(4-cyanatobenzyl) cyclohexane (BCC)

The synthesis of 1, 3-bis (4-cyanatobenzyl) cyclohexane (BCC) is as follows; CDD was dissolved in dry acetone under nitrogen atmosphere and then the solution of cyanogen bromide in acetone was added, followed by the slow addition of triethyl amine at -15°C. Then the temperature was slowly raised to room temperature and stirred for 1h. Subsequently, the reaction mixture was filtered and the filtrate was added to cold water, the precipitate thus obtained was filtered and washed several times with water and dried for 12h at 40°C to yield 88% pale yellow solid product.

FTIR (KBr cm^{-1}): 2923 (symmetric stretching), 2854 (cyclohexyl CH_2 asymmetric stretching), 2238 (CN vibration stretching).

^{1}H NMR (DMSO-d_6, δ, ppm): 7.45-7.33 (aromatic protons), 2.49-2.39 (methylene protons), 1.65-1.20 (cycloaliphatic protons).

^{13}C NMR (DMSO-d_6, δ, ppm): 150.91, 139.78, 131.28, 115.26 (aromatic carbon), 108.98 (OCN), 51.32 (methylene carbon) 34.15, 26.02, 24.44 (cycloaliphatic carbon).

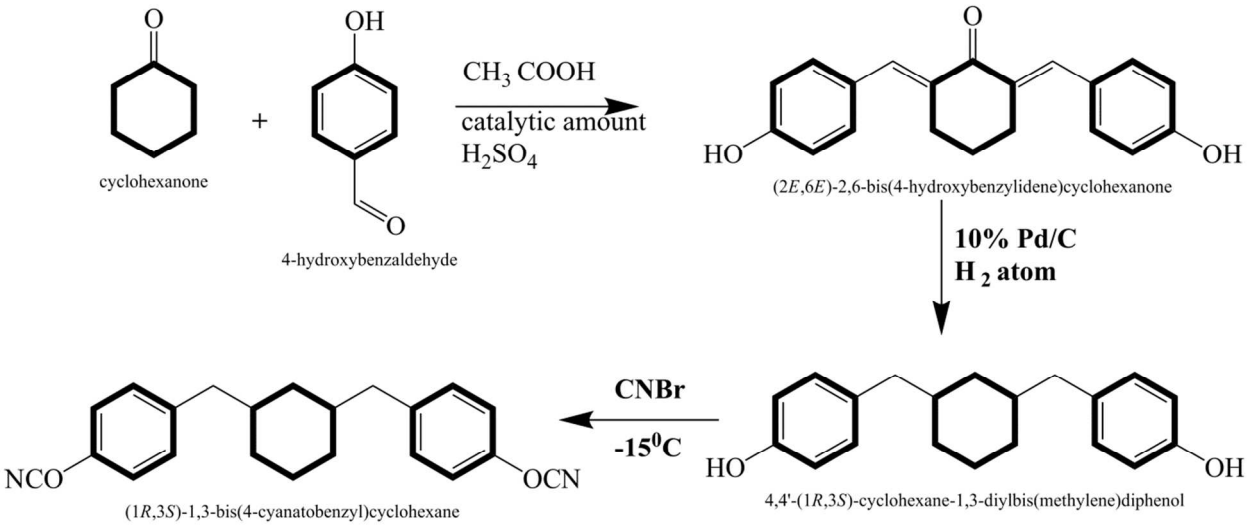

Scheme.1 Preparation of BCC cyanate ester

Synthesis of MCM-41 and functionalization of MCM-41 (FMCM-41)

MCM-41 was synthesized as per the previous report[16,17] is as follows; to an aqueous solution of sodium trisilicate, catalytic amount of cetyltrimethylammonium bromide (CTAB) was added drop by drop at room temperature under vigorous stirring and continued for 1h. Then the resultant gel was heated for 24h at 100ºC. The jelly mass was cooled to room temperature, and the pH was adjusted to 10 with acetic acid and it was further heated for 48h at 100ºC. The pH adjustment and subsequent heating were repeated, and the precipitated MCM-41 product was collected by filtration. The product was washed with ethanol and calcined in air at 550ºC. After that, MCM-41 was functionalized with GPTMS (FMCM-41) as per the procedure reported[18]; to a suspended solution of MCM-41 in ethanol, GPTMS was added and sonicated for 1h and then the mixture was refluxed for 24h. After that the precipitate was filtered and washed with cold ethanol and dried at 70^{o}C under reduced vacuum to obtain FMCM-41.

Development of BCC/FMCM-41 nanocomposites

The BCC/FMCM-41 nanocomposites with different concentration of FMCM-41 (1, 3, 5, 7 and 10%) were prepared according to the (Scheme 2); the solution of FMCM-41in THF was

sonicated for 15 minutes, subsequently BCC was added to that clear solution and stirred for 15 minutes at 30°C. The resulting viscous solution was poured into a respective glass mold and allowed to evaporate the solvent at 50°C for 3h and then the temperature was raised slowly to 210°C at the heating rate of 20°C /h. After that the cured films were removed and preserved for further characterization.

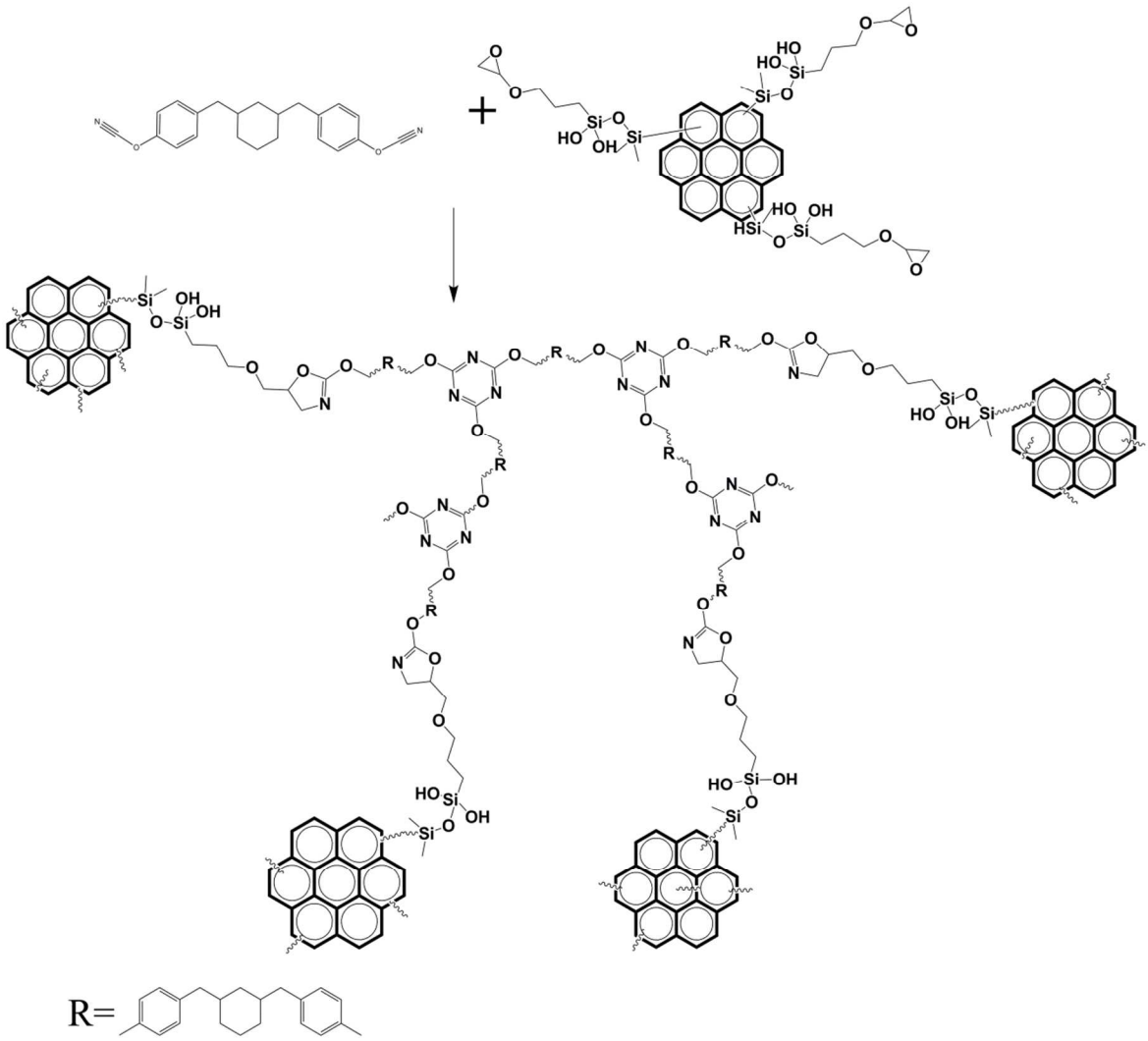

Scheme.2 Preparation of BCC/FMCM-41 polymeric nanocomposites

Characterization

FTIR spectroscopic measurements were conducted on a Bruker (TENSOR 27) using KBr pellet method. ^{1}H and ^{13}C NMR spectra were recorded on a Bruker 500 NMR spectrometer. Thermogravimetric measurements carried out on a Q500 Hi-Res TGA from TA instruments

thermo gravimetric analyzer. The samples (about 10 mg) were heated from ambient temperature to 800ºC under a continuous flow of nitrogen (20 mL/min), at a heating rate of 10ºC/min. The calorimetric analysis of the nanocomposites were performed on a Netzsch DSC-200 differential scanning calorimeter at a heating rate of $10^{\circ}C\ min^{-1}$ under nitrogen atmosphere. The X-ray photoelectron spectroscopic analysis of the samples were carried out using a JEOL JPS-9200 photoelectron spectrometer with a mono-chromatized Al-Kα X-ray source operated at 12 kV and 20 mA.

High resolution transmission electron microscope (HRTEM) analysis was carried out on TECNAI-G^2 (model T-30) at an accelerating voltage of 300 kV. Scanning electron microscope (SEM) measurements were performed using VEGA 3 TESCAN scanning electron microscope. The piece of film fixed in the surface of double-sided adhesive tape, and the film was sputtered with gold prior to SEM observation. Dielectric constant was determined by Broad band Dielectric Spectrometer (BDS), NOVOCONTROL Technologies GmbH & Co. (model Concept 80) at 30ºC in the range of 100 Hz to 1MHz.

Results and discussion

To investigate the dielectric properties of cyanate ester matrices and composites (Scheme 2), less polar aliphatic based cyanate ester was designed and its molecular structure was confirmed by the NMR and FTIR spectral analysis. For the synthesis of BCC three step processes were used, first BHC was synthesized and then the BHC was reduced to get cyclohexyl branched aliphatic chain bridged phenolic diol (CDD). Finally, CDD was treated with cyanogen bromide to get BCC (Scheme 1). Fig. 1a presents the ^{1}H NMR spectral data of CDD. The appearance of peaks at 9.14 ppm was attributed to aromatic OH group and the peaks appeared in the range from 6.93 to 6.61 ppm were correspond to the aromatic protons. The formation of cyclohexane branched aliphatic chain linked aromatic diol was confirmed by the appearance of peaks in the range from 2.63 to 2.46 ppm and 1.89 to 1.16 ppm, which represent for respective aliphatic shielded region. Further the successful formation of cyanate ester was confirmed by FTIR, ^{1}H and ^{13}C NMR spectral data. Fig. 1b shows the ^{1}H NMR spectra, the disappearance of respective aromatic OH peak and the retaining of peaks in the ranges from 7.45-7.33 ppm (aromatic protons), 2.49-2.39 ppm (methylene protons) and 1.65-1.20 ppm (cycloaliphatic protons) indicate the formation of cyanate ester. Furthermore the structure

elucidation was also confirmed by ^{13}C NMR (Fig. 1c), the peak appeared at 108.9 was associated with OCN and also the aromatic and aliphatic peaks exhibit in the ranges of 150.91 to 139.8 ppm and 51.3 to 24.4 ppm respectively. In addition, the FTIR spectral data (Fig. 1d) also used ascertain the OCN formation, the new absorption band at 2238 cm^{-1} was attributed to OCN and the respective aliphatic vibration bands were observed in range of 2854 to 2923 cm^{-1} indicate the successful formation of BCC.

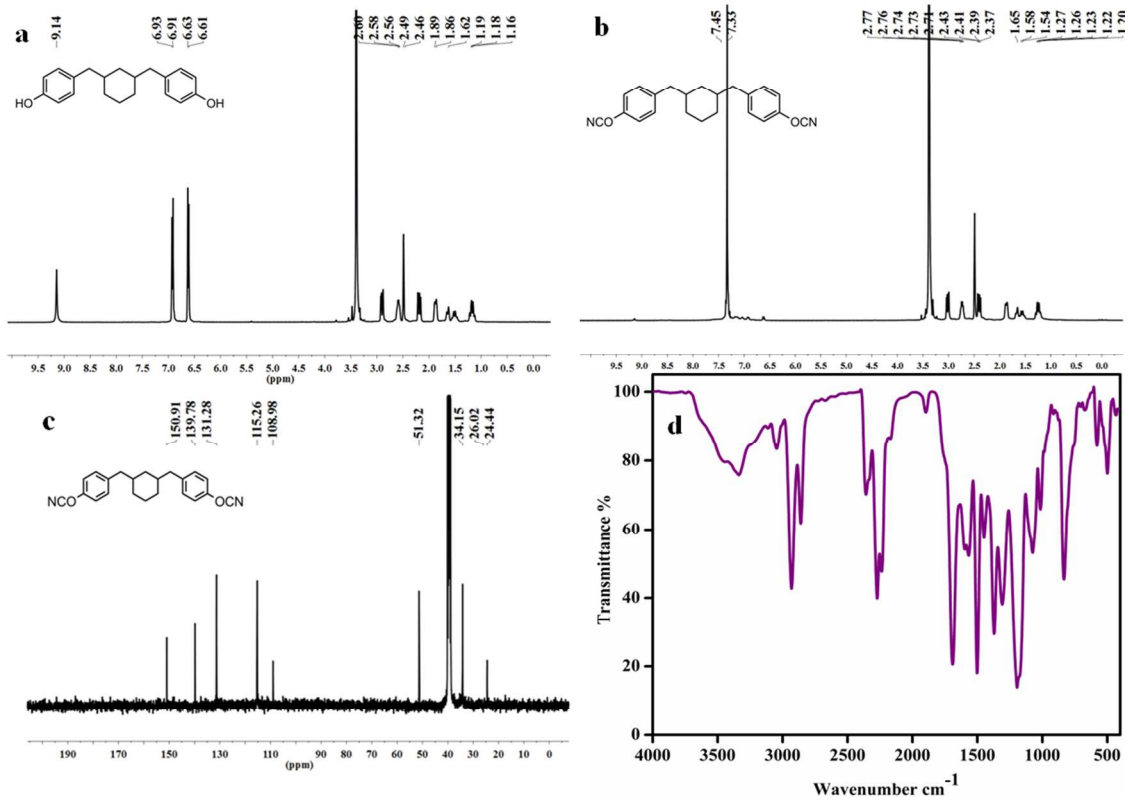

Fig.1 (a) ^{1}H NMR spectrum of CDD,(b) ^{1}H NMR spectrum BCC,(c) ^{13}C NMR spectrum BCC and (d)FTIR spectrum of BCC monomer

The molecular structure of MCM-41and FMCM-41 was confirmed by FTIR spectra (Fig. 2). FTIR spectra show the bands at 1087 cm^{-1} and 792 cm^{-1} are correspond to asymmetric and symmetric stretching vibrations of Si-O-Si bonding respectively. The broad absorption band at 3500 cm^{-1} was attributed to the hydroxyl group of MCM-41. In addition, the GPTMS functionalized FMCM-41 was confirmed by the appearance of new bands at 2933 cm^{-1} and 2856 cm^{-1} represent asymmetric and symmetric stretching modes of CH_2 group respectively and the band appeared at 934 cm^{-1} indicates the presence of glycidyl group, which confirm the successful functionalization of FMCM-41.

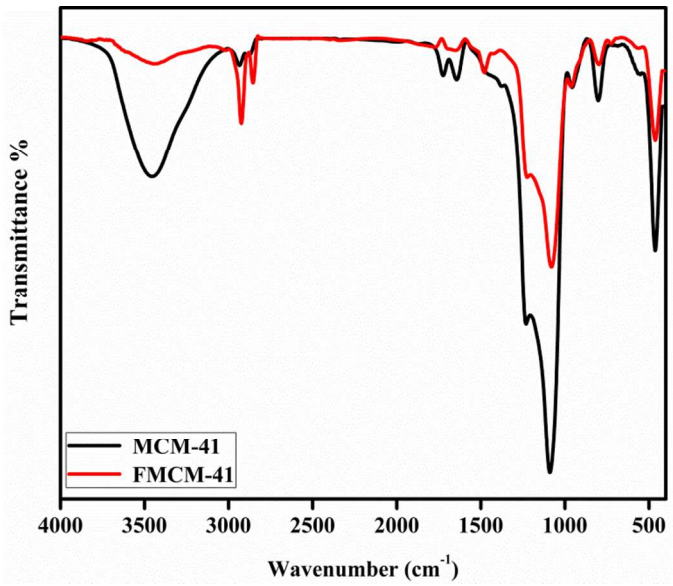

Fig.2 FTIR spectra of MCM-41 and GPTMS functionalized FMCM-41

The cured BCC/FMCM-41 nanocomposites were characterized by FTIR spectra. S1 shows the disappearance of bands at 2252 cm^{-1} (the –OCN group of the cyanate ester) and 943 cm^{-1} (the glycidyl group of FMCM-41) and the appearance of band at 1645 cm^{-1} (oxazoline ring) indicate the successful incorporation of FMCM-41 through covalent bond by the cyclic oxazoline ring formation between OCN group of cyanate ester and glycidyl group of FMCM-41. Further the appearance of bands at 1085 cm^{-1} and 1365 cm^{-1} are associated with Si-O-Si linkages and the triazine ring respectively[3], which indicates the successful formation of triazine rings by the self polymerization of OCN. The combination of triazine and oxazoline rings with aliphatic chain and porous silica materials facilitate in the reduction of dielectric constant of nanocomposites.

The various chemical bonds of polymer nanocomposites have their own binding energies and it can be evaluated by X-ray photoelectron spectroscopy (XPS), from that the formation of chemical structure of the polymer composites were examined. Fig.3a shows the XPS survey spectra of BCC /10% FMCM-41, from which it could be clearly observed that the binding energies of elemental peaks at 283eV, 531eV, 398eV, 101eV are corresponds to C1s, O1s, N1s, and Si2p respectively[19,20]. Fig.3b-d shows the deconvulation peaks of individual elements with the characteristic binding energies and it could be supported by the earlier reports. Consequently,

the deconvolued peaks infer the existence of different kinds of bonds in the polymer composites with typical binding energies. Fig.3b shows the deconvolution of C1s signal into three peaks, the major peak at 284.4 eV corresponds to C-C, C=C and Si-C bonds and the second major peak at 285.6 eV associated to the C-O-C bonds. Subsequently, the third peak at 288.6 represents N=C-O bonds of oxazoline ring indicates the successful incorporation of FMCM-41 through covalent bonds[21]. Fig. 3c shows the deconvolution of N1s signal into two peaks, the peak at 398.4 was assigned to the contribution of C=N-C bonds of triazine ring in the polymer composites infer the cyanate esters were self polymerized to form polycyanurate and the peak at 404.5 eV represent the characteristic shake up satellite peak which was raised by π - π* transitions in aromatic groups[22]. In addition, the characteristic O1s signal was deconvoluted into two peaks; the major peak (Fig. 3d) at 530.9 eV corresponds to C-O and other one exhibit at 532.2 eV was assigned to Si-O-Si bonds. From these observations it could be clearly ascertained the successful formation of BCC/FMCM-41 polymer nanocomposites through strong covalent bonds.

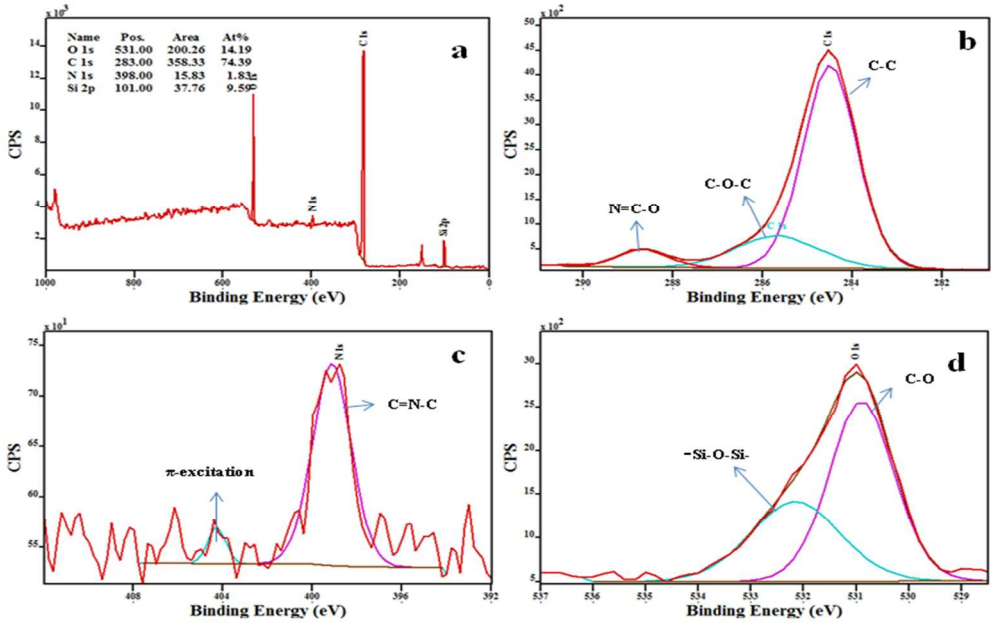

Fig.3 XPS sectrum of BCC/10%FMCM-41 polymeric nanocomposites

The well defined surface microstructure of the polymer nanocomposites can be observed by Scanning electron microscopy (SEM). Fig. 4 shows the SEM images of the surface of the neat and 10% FMCM-41 reinforced cyanate ester composites, from which it could be clearly observed that the smooth surface indicates the homogeneous polymerization of cyanate ester.

Although the homogeneous distribution of light spots in the BCC/FMCM-41 polymer composites indicate the covalently bonded FMCM-41 with the cyanate ester through the oxazoline ring and influence the formation of homogeneous surface. Fig. 4c describes the results of Si-mapping of the 10% FMCM-41 composite and demonstrates the uniform distribution of MCM-41 over the surface. Thus, the distinguishable microstructures of neat and their composites indicate the existence of silica particles well coordinated with cyanate esters in their composites which could contribute to sustainable thermal stability. However, it could not describe any dielectric features of the polymer composite films and it need to be studied about the internal microstructure of the films.

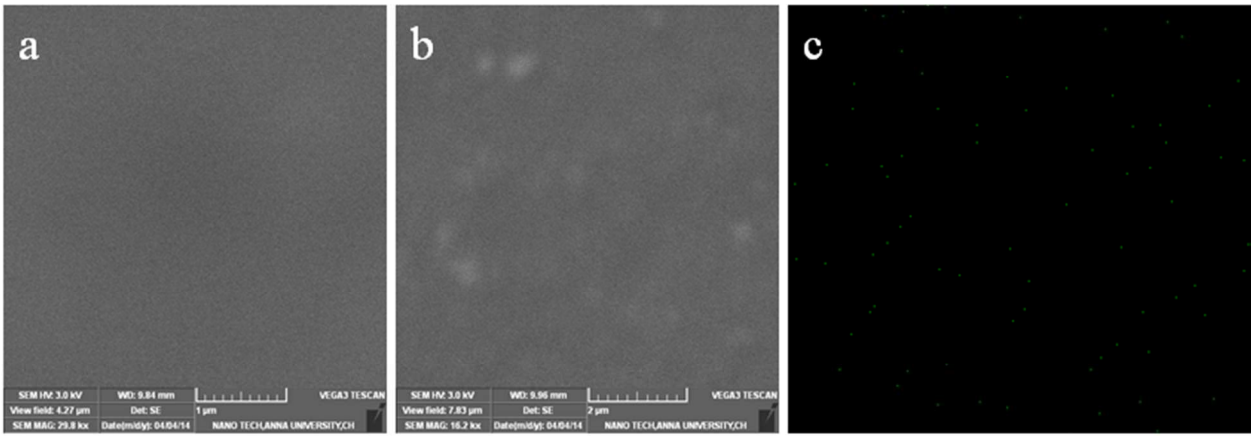

Fig.4 SEM images (a) BCC polymer (b) BCC/10%FMCM-41 and (c) Si maping BCC/10%FMCM-41 polymeric nanocomposite

In order to understand the internal microstructure of composites with varying weight percentages of FMCM-41 were studied by high resolution transmission electron microscope (HRTEM). Fig. 5a,b and Fig. 5c,d shows the HRTEM images of MCM-41 and BCC/10% FMCM-41 composites, respectively. Fig. 5a,b shows the porous nature of the as prepared MCM-41 materials. Subsequently, the different weight percentages of FMCM-41 were incorporated into the cyanate ester resin to form cyanate ester nanocomposites. From Fig. 5c,d it can be seen that the porous silica nanoparticles surrounded by cyanate ester with distinct distances. In addition, the uniform distribution of porous silica segments in the composites provides an ordered air/vacuum in the appropriate places. Thus, the definite internal microstructure clearly demonstrate that the existence of pores which contributes to the reduction in the value of dielectric constant of the composites.

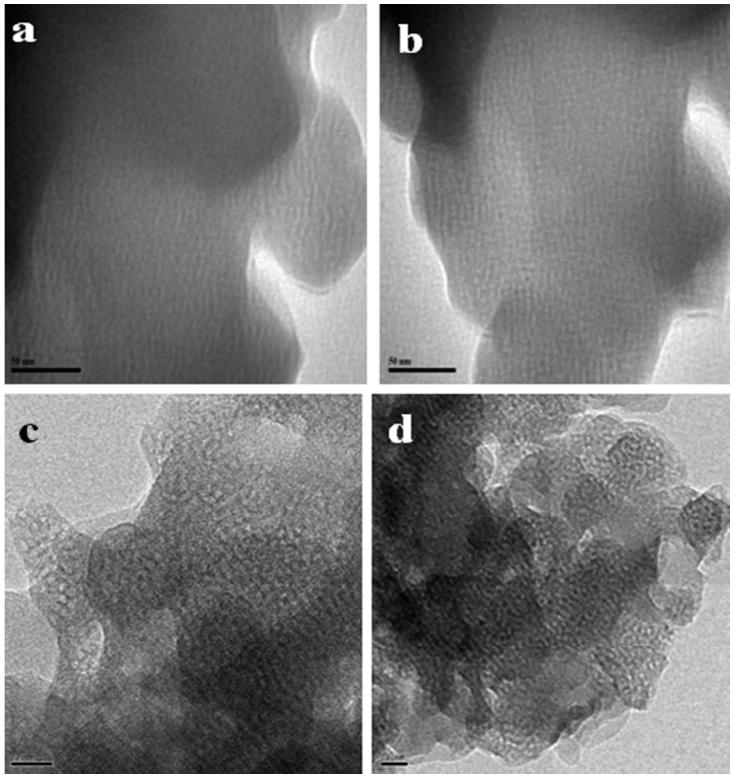

Fig.5 HRTEM image of MCM-41 and BCC/10% FMCM-41 polymeric nanocomposite

Thermal stability of the BCC/FMCM-41 composites has been ascertained by the thermogravimetric analysis. Fig.6 shows the TGA curve of different weight ratio of BCC /FMCM-41 composites. It can be seen that the increasing weight percentages of FMCM-41 increases the thermal stability of the resulting polymer composites and the higher percentages of 10% of mesoporous silica exhibit better thermal stability than that of neat sample indicate the existence of rigid siloxane and the strong covalent bond of Si-O-Si skeleton contributes to an enhanced thermal stability of the composites. In addition, the gradual increment of char yield suggests that the presence of triazine ring and oxazoline linked silica materials converted to form thermally stable rigid graphene like structure with silica layers at higher temperature[23]. In detail, the initial weight loss of material below 200^{o}C is probably due to the removal of residual solvent and adsorbed moisture. The major weight loss observed above 300^{o}C is associated with the decomposition of polymer network and finally to yield residual chair at 800^{o}C and are presented in Table 1. Moreover, higher the decomposition temperature and char yield indicate the higher thermal stability of the polymer composites, which suggested the utility of these composites in the field of microelectronics as interlayer materials. S2 shows the DSC profile of neat BCC and

BCC/10% FMCM-41 composites. For the neat BCC exhibits the broad exothermic peak maximum at 210^{o}C indicate the formation of polycyanurate by the polymerisation of cyanate ester which is an exothermic reaction. The BCC/10% FMCM-41 shows the absence of exothermic peak indicate the occurence of complete polymerised composites. The existance of absolute polymerisation illustrates the uniform structure formation.

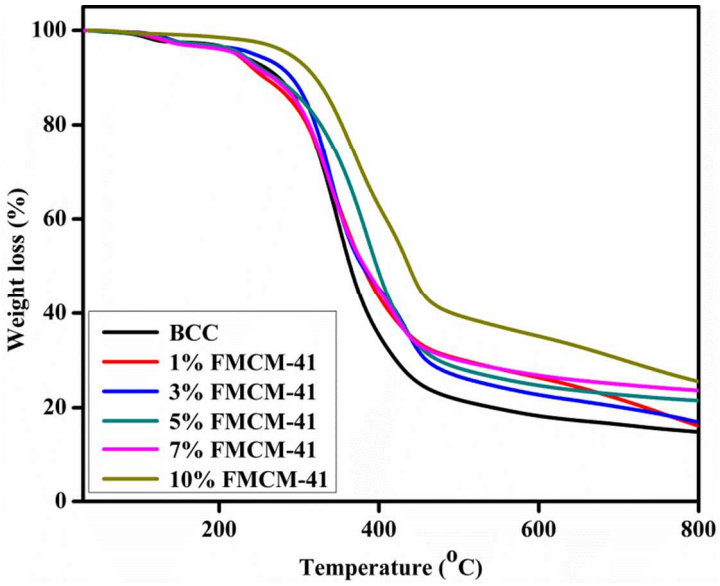

Fig.6 Thermogram curve BCC/FMCM-41 polymeric nanocomposites

Microelectronics devices need a most desirable lower dielectric constant material as interlayer, so it warrants the development of such novel materials. Recently, the researchers have been made many efforts towards the reduction of the values of dielectric constant of the polymeric materials due to their characteristic physico chemical properties. Thus, the lowest values of dielectric constant materials (below 2) have potential applications in electronic devices. In order to obtain the potential dielectrics, porous silica based polycyanurate polymer composites were prepared by the polymerization of cyanate ester with varying weight percentages of mesoporous materials. Fig. 7, S3 and Table 1 shows the dielectric constant (k) and dielectric loss of the neat and composite materials. Fig. 7 shows the decreasing trend of dielectric constant with increasing FMCM-41 content due to the increases of porous nature of silica material which provokes air in the composites. Fig. 8 presents the log-log form of frequency dependency of dielectric constant for BCC/FMCM-41 nanocomposites. From Fig. 8 the significant variation on dielectric constant with the frequency as well as FMCM-41 concentration can be seen. The

absence of peaks (Fig. 8) indicates homogeneous polarization of the nanocomposites. Over the measured frequency region, plateau variation in dielectric constant was observed in both lower and higher frequency region which demonstrates that the low relaxation and less interfacial polarization of the matrix[24,25]. In addition, the HRTEM images were clearly shows the existences of pores, which suggest that the existing pores mainly contribute to the reduction of the dielectric constant of the material. The neat polycyanurate exhibit the value of dielectric constant of 2.98 which is the lower value than that of the previously reported polycyanurate. This may be due to the presence of more number of less polarizable aliphatic CH_2 groups in the polymer composites. Moreover, the non polar aliphatic chain intrinsically reduces the dipoles between the electrodes and significantly reduces the value of dielectric constant throughout the matrix, because the reduction of polarization between the electrodes influences to the reduction of capacitance and hence reduces the value of dielectric constant. In addition, the increasing weight percentages of FMCM-41 gradually decreases the value of dielectric constant of 1.98 for 10wt % of FMCM-41 beyond 10wt% to FMCM41 the reverse trend in the value of dielectric constant was noticed due to the agglomeration of mesoporous materials in the polymer composites which may reduce the homogeneous porosity of the composites. The dielectric loss is one the most important factor in the interlayer dielectrics which could contribute to the power consumption in the microelectronics. Moreover, the lowest value of dielectric loss was mainly contributes to the reduction of current leakages and to avoid cross talk. S3 shows the dielectric loss spectrum of neat and the varying weight percentages of FMCM-41. The neat polycyanurate exhibits the tangent loss value of 0.0233 and the lowest tangent loss value of 0.0092 was observed for BCC /7% FMCM-41 polymer nanocomposites indicate that these types of composite materials can be employed as a potential candidate for the next generation microelectronics.

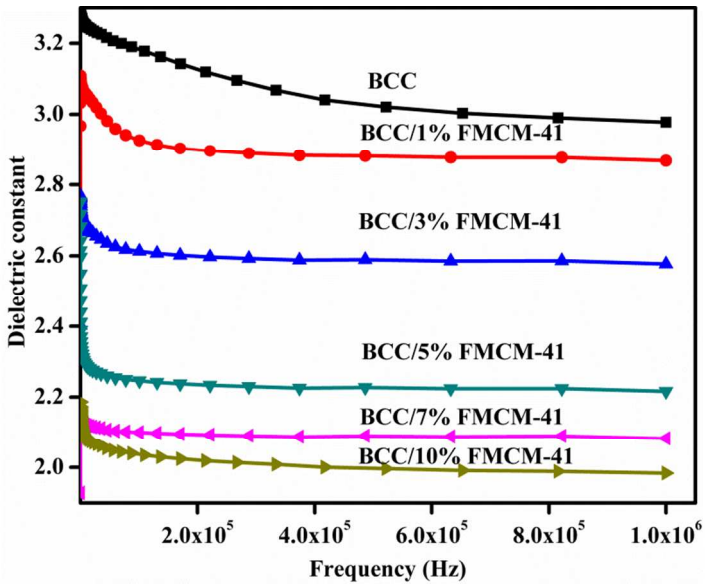

Fig.7 Dieletric constant of BCC and BCC/FMCM-41 polymeric nanocomposites

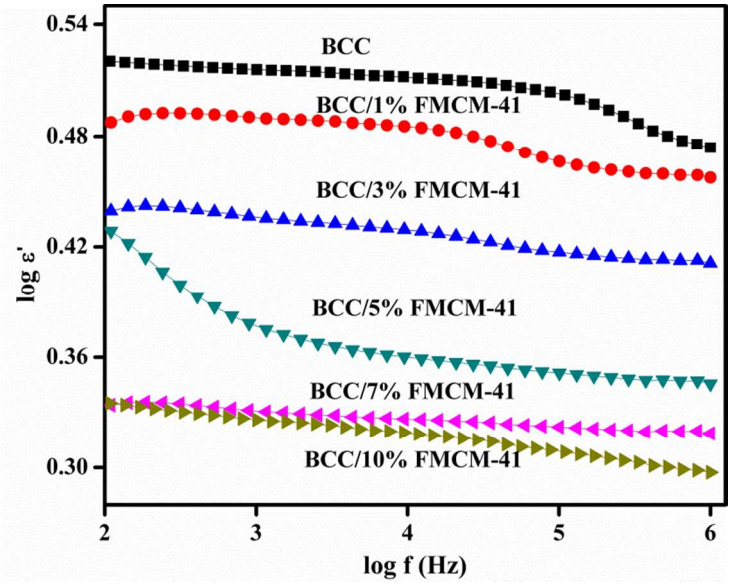

Fig.8 Log-log polt dieletric constant of BCC and BCC/FMCM-41 polymeric nanocomposites

Table.1 Thermal and dielectric properties of BCC/FMCM-41nanocomposites

Sample	Char yield 800ºC (%)	Dielectric constant	Tangent loss
BCC	14.88	2.97	0.0233
BCC/1%FMCM-41	16.18	2.87	0.0103
BCC/3%FMCM-41	16.94	2.58	0.0102
BCC/5%FMCM-41	21.49	2.22	0.0102
BCC/7%FMCM-41	23.6	2.08	0.0092
BCC/10%FMCM-41	25.55	1.98	0.0140

Conclusion

With a view to reduce the value of dielectric constant, a new class of cyclohexyl branched aliphatic chain bridged phenolic cyanate ester has been synthesized and subsequently polycyanurate composites with varying weight percentages of glycidyl silane functionalized MCM-41were developed. The existence of less polar aliphatic groups in the cyanate ester monomer skeleton significantly reduced the value of dielectric constant in the neat polycyanurate; however it is not sufficient to meet the low k requirements. Hence, it was further reduced by the incorporation of mesoporous functionalized FMCM-41, the homogeneously dispersed composites of BCC/10% FMCM-41 exhibits the lowest value of dielectric constant of 1.98 at 1MHz. In addition, the dielectric loss was also decreased with increasing mesoporous FMCM-41 content. Further the thermal stability of polymer composites was also considerably increased with increasing Si-O-Si linkage. Data resulted from different experimental studies, it is suggested that the newly developed class of skeletal modified cyanate ester polymer composites can be used as potential insulation material for microelectronic applications.

Acknowledgment

The authors thank DST (Nanomission), SR/NM/NS-18/2010, New Delhi, Govt. of India., for the financial support. The authors also thank Dr. K. Gunasekaran, and Mr. M. Kesavan, Department of Crystallography and Biophysics for providing NMR facility and Dr. S. Balakumar, National Centre for Nanoscience and Nanotechnology, University of Madras, for providing HRTEM facility.

REFERENCES

1. B. D. Hatton, K. Landskron, W. J. Hunks, M. R. Bennett, D. Shukaris, D. D. Perovic and G.A. Ozin, *Materials today*, 2006, **9**, 22-31.

2. R. D. Miller, *Science*, 1999,**286**, 421-423.

3. S. Devaraju, M.R. Vengatesan, M. Selvi, J.K. Song and M. Alagar*, Microporous and Mesoporous Materials*, 2013,**179**, 157–164.

4. R. Sasi kumar, M. Ariraman and M. Alagar, *RSC Adv*, 2014, **4**, 19127-19136.

5. M. R. Vengatesan, S. Devaraju, K. Dinakaran and M. Alagar, *J. Mater. Chem*, 2012, **22**, 7559-7566.

6. S. Baskaran, J. Liu, K. Domansky,N. Kohler, X.Li, C. Coyle, G. E. Fryxell, S. Thevuthasan and R. E. Williford, *Adv. Mater.* 2000, **12**, 291-294.

7. F. Goethals, I. Ciofi, O. Madia, K. Vanstreels, M. R. Baklanov, C. Detavernier, P. Van Der Voorta and I. Van Driessche, *J. Mater. Chem*., 2012, **22**, 8281-8286.

8**.** S. Devaraju, P. Prabunathan, M. Selvi and M. Alagar, *Frontier in chemistry,* 2013, **1**, 1-10.

9. D. Shamiryan, T. Abell, F. Iacopi and K. Maex, *Materials today,* 2004, **7**, 34-39.

10. E. Aram and S. Mehdipour-Ataei*, J. Appl. Polym. Sci*. 2013, **128**, 4387-4394.

11. Z. Geng, M. Huo, J. Mu, S. Zhang, Y. Lu, J. Luan, P. Huo, Y. Dua and G. Wang, *J. Mater. Chem. C*, 2014, **2**, 1094–1103.

12. B. Yameen, H. Duran, A. Best, U. Jonas, M. Steinhart and W. Knoll, *Macromol. Chem. Phys.*, 2008, **209**, 1673–1685.

13. M. Laskoski , D. D. Dominguez and T. M. Keller, *Polymer*, 2006, **47**, 3727–3733.

14. G. Zhan, L. Zhao, S. Hu, W. Gan, Y. Yu and X.Tang, *Polymer Engineering And Science*, 2008, **48**, 1322–1328.

15. X. Fang, L. Fang, S. Gou and L. Cheng, *Bioorg. Med. Chem. Lett*., 2013, **23**, 1297–1301.

16. Z. Liu, Y. Sakamoto, T. Ohsuna, K. Hiraga, O. Terasaki, C. H. Ko, H. J. Shin and R. Ryoo, *Angew. Chem*, 2000, **112**, 3237-3240.

17. A. Kalilur Rahiman, K. Shanmuga Bharathi, S. Sreedaran, K. Rajesh and V. Narayanan, *Inorganica Chimica Acta*, 2009, **362**,1810–1818

18. M. R. Mello , D. Phanon , G. Q. Silveira, P. L. Llewellyn and C. M. Ronconi, *Microporous and Mesoporous Materials*, 2011, **143**,174–179.

19. L. Zhang, A. Chatterjee, M. Ebrahimi, and K. T. Leung, *J. Chem. Phys.*, 2009, **130**, 121103 .

20. K. Ellinas, S.P. Pujari, D. A. Dragatogiannis, C.A. Charitidis, A. Tserepi, H. Zuilhof, and E. Gogolides, *ACS Appl. Mater. Interfaces*, 2014, **6**, 6510−6524

21. E.S. Kim, G. Hwang, M. G. El-Din and Y. Liu, *Journal of Membrane Science ,* 2012, **394–395,** 37– 48.

22. A.P. Dementjev, A. de Graaf, M.C.M. van de Sanden, K.I. Maslakov, A.V. Naumkin and A.A. Serov, *Diamond and Related Materials,* 2009, **9**, 1904-1907.

23. R. E. Lyon, R. N. Walters and S. Gandhi, *Fire Mater,* 2006, **30**, 89–106.

24. M. Ariraman, R. Sasi kumar and M. Alagar, *J. Appl. Polym. Sci.,* 2014, **131**, 41097 (1 of 10).

25. R. Popielarz, C. K. Chiang, R. Nozaki, J. Obrzut, *Macromolecules*.,2001, **34**, 5910-5915.